Results in Engineering 19 (2023) 101297

Contents lists available at ScienceDirect

Results in Engineering

journal homepage: www.sciencedirect.com/journal/results-in-engineering

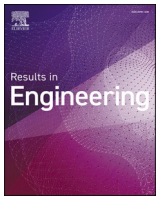

Sensor system for precision agriculture smart watering can

Anika Rabak [a], Kiranmai Uppuluri [b], Fabiane Fantinelli Franco [c], Naveen Kumar [a], Vihar P. Georgiev [a], Caroline Gauchotte-Lindsay [c], Cindy Smith [c], Richard A. Hogg [a], Libu Manjakkal [a,d,*]

[a] Electronic and Nanoscale Engineering, James Watt School of Engineering, University of Glasgow, Glasgow, G12 8LT, UK
[b] Łukasiewicz Research Network—Institute of Microelectronics and Photonics, Kraków Division, ul. Zabłocie 39, 30-701, Kraków, Poland
[c] Water and Environment Group, Infrastructure and Environment Division, James Watt School of Engineering, University of Glasgow, Glasgow, G12 8LT, UK
[d] School of Computing and Engineering & the Built Environment, Edinburgh Napier University, Merchiston Campus, EH10 5DT, UK

ARTICLE INFO

Keywords:
Electrochemical sensor
Precision agriculture
Metal oxide
Soil monitoring
Tap water monitoring

ABSTRACT

The expansion of precision agriculture technology from commercial agriculture to home gardening is highly important due to its economic and health benefits, delivered through a new way of crop production. Additionally, it offers physiological and psychological benefits to the gardeners. The soil degradation and lack of knowledge among gardeners related to the properties of both soil and the pouring water chemical contents results in less efficient production from home plants. In this work, we proposed a new connected sensor system in which smart watering can connect to a wireless sensor network for soil analysis along with the properties of water. The soil condition was measured using thick film pH and moisture sensors. The sensitivity of the pH sensor is 53 ± 2 mV/pH for RuO_2 vs Ag/AgCl electrode and is 42 ± 1.26 mV/pH for RuO_2 vs carbon in the range of pH 3–8. Depending on the soil properties, the sensors integrated watering can create a suitable pH solution by automatically, mixing the alkaline/acidic solution stored in separate containers in the watering can. This prepared pH-controlled water is then deposited into the plant by the user. Online monitoring of both soil and pouring water chemical content support the gardener to grow plants sustainably.

1. Introduction

The tremendous increase in population has resulted in a 60% growth in food production to ensure food security for the growing population [1]. Additionally, climate change and deforestation also have the potential to affect both crop yield and quality [2–4]. Land degradation from agricultural land expansion can lead to climate change, therefore a thorough revaluation of effective commercial agriculture is necessary. For effective food production, the yield and well-being of the plants strongly depend on soil properties, temperature, and the fertilizer/pesticides used for plant growth. However, the currently available major soil monitoring systems focus on commercial agriculture applications to check the soil properties. Even though many studies were reported on sensors and online monitoring system for wearables and environmental monitoring [5–8], the digitalization of agriculture and aquaculture studies are limited. Especially the number of studies on a monitoring system aimed at indoor gardening is limited. For monitoring and improved working conditions in farming/gardening [9–11], the digitalization of agriculture will have huge advantages which will enable environmental sustainability and economic growth. The lack of advanced sensors which can monitor the nutrients required for the growth and good health of crops including house plants demands advanced sensor systems for simultaneous analysis of the soil and the water. These sensors could determine the chemical and bio-chemical processes occurring in the soil and provide detailed information on the nutrients of the soil. The major advantage of online monitoring of nutrients in plants is to support inexperienced gardeners and people who are unable to properly care for their plants due to illness or disability.

The precision agriculture incorporation with the Internet of Things (IoT) provides real-time and remote monitoring of the conditions and requirements of crop growth [12,13] for crop production. In commercial agriculture, variables such as pH, moisture, temperature, and nutrients of the soil as well as weather conditions are required to be monitored. Some recent works include soil-based pH and Ca^{2+} monitoring using ion-sensitive probes [14], determination of ions (pH, Ca^{2+}, K^{+} and NO^{3-}) based on ion-sensitive field effect transistors (ISFETs) [15] and

* Corresponding author. School of Computing and Engineering & the Built Environment, Edinburgh Napier University, Merchiston Campus, EH10 5DT, UK.
E-mail address: L.Manjakkal@napier.ac.uk (L. Manjakkal).

https://doi.org/10.1016/j.rineng.2023.101297
Received 18 May 2023; Received in revised form 4 July 2023; Accepted 11 July 2023
Available online 12 July 2023

ISFET for multi-ion detection (H^+, Na^+, and K^+) with deep neural network for accurate data [16]. For nutrient monitoring, the pH value of the soil is considered a key variable as it is the determining factor in many chemical and biochemical processes [14,17–20]. Most importantly, soil pH regulates nutrient availability by controlling the chemical form of nutrients and their chemical reactions. As such, soil pH has a great effect on crop yield and plant growth [19]. Many nutrients including nitrogen, phosphorus, potassium, sulphur, calcium, magnesium, manganese, boron, copper, zinc, iron, and molybdenum are present in soil which determines its acidity or alkalinity [21,22]. In nature, soil pH is greatly affected by climate, as soils in humid conditions are more acidic, whereas drier soils are more alkaline [19]. In addition to this, rainfall also affects the soil pH, with soils becoming more acidic over time due to the pH 5.7 of clean rainwater [19]. Indoor plants, however, are usually watered using tap water, and thus, their pH remains neutral with a value of ~ 7. Moreover, different plants have different requirements when it comes to soil pH and the availability of nutrients. Hence to estimate the soil pH in agriculture an advanced sensing system is required which can monitor simultaneously the pH of soil and water. The interference of other chemicals due to the various nutrients present in the soil can influence the pH sensing performances. Therefore, multi-sensing probe-integrated systems will be an advanced method for this, which can monitor multiple parameters simultaneously and better analyze the data. Fig. 1a outlines the pH requirements of common house plants. Because of this, soil pH is a determining factor in which plants can thrive in different fields. In addition to this, similar to soil monitoring, hydroponic plants need the chemical properties of the supplied water to be cross-checked for sustainable and healthy growth. Even though pH and other ion-sensitive electrodes were reported for soil monitoring [14], simultaneous determination of the soil pH and the pouring water pH has not been thoroughly discussed.

In this work, we developed a thick film potentiometric pH sensor for real-time monitoring of soil and tap water (Fig. 1b and c). The pH sensor was fabricated using a screen-printed RuO_2 based sensitive electrode (SE) and thick film Ag/AgCl reference electrodes (RE). In addition, we also investigated the applicability of carbon printed electrode as a RE instead of Ag/AgCl. Through the design of a printed circuit board (PCB) with Arduino Uno board we developed a prototype for online monitoring of soil and water pH and humidity. Finally, we designed a new smart watering can, which can monitor water pH and adjust it through controlled addition of acidic/alkaline solution, as shown in Fig. 1c. The schematic of the system architecture is presented in Fig. 2. We carried out a detailed characterization of the sensor to understand the sensing performance and electrochemical reaction of RuO_2 vs Ag/AgCl and RuO_2 vs carbon using potentiometry, cyclic voltammetry (CV) and electrochemical impedance spectroscopic analysis (EIS). The sensor performances in $Ca_3(NO_3)_2$, KCl, $MgCl_2$, NaCl and NH_4NO_3 solution were also tested to understand selectivity of the pH sensor. By automatically calculating the amount of water to be deposited in the potted plant and adjusting for chemical parameters of the soil/water according to the plant type, this advanced sensing system will lead to a successful home garden, without requiring much knowledge or time from the gardeners.

2. Methods

2.1. Sensors fabrication and characterization

In this work, the thick film potentiometric pH sensor was fabricated using screen-printing method. RuO_2 paste (ESL) was used as a SE and is printed on the top of Ag conductive electrode and its fabrication procedure was similar to our previous work [23,24]. For the REs, we used thick film Ag/AgCl RE comparable to commercial Ag/AgCl glass electrodes. AgCl paste (paste (JESC-7713AgCl, JE Solutions Consultancy, UK) hand printed on the top of screen-printed Ag electrode. After printing the film was heat treated at 100 °C for 1hr. We also investigated the performances of the sensor using carbon printed electrode as a RE without any AgCl or reference membrane. The carbon paste (Sun-Chemical) was used for printing the electrode on a polyvinyl chloride substrate. After printing, the sample was heat treated at 80 °C for 30 min. The moisture content of the sensors was measured using a capacitive probe-based humidity sensor i.e., DFRobot. Soil monitor sensor and its value represented as an integer.

Here, prior to testing the sensor in soil, we calibrated the sensor in dilute HCl (1 M) and dilute KOH (1 M) solutions. Electrode sensitivity was determined by sweeping the electrode through different pH values and measuring the resulting electromotive force (emf). The electrodes were placed in a glass beaker and submerged, initially, in tap water. For the first set of experiments, the potential difference emf between the SEs and the REs was measured using a multimeter. The potential difference was measured for pH values 4–8, as this is the pH range suitable for most plants. For testing in soil, the pH of the solution was also changed by dropping small amounts of commercial phosphoric acid (81%) to lower the pH value, and potassium hydroxide (25%) to increase the pH value.

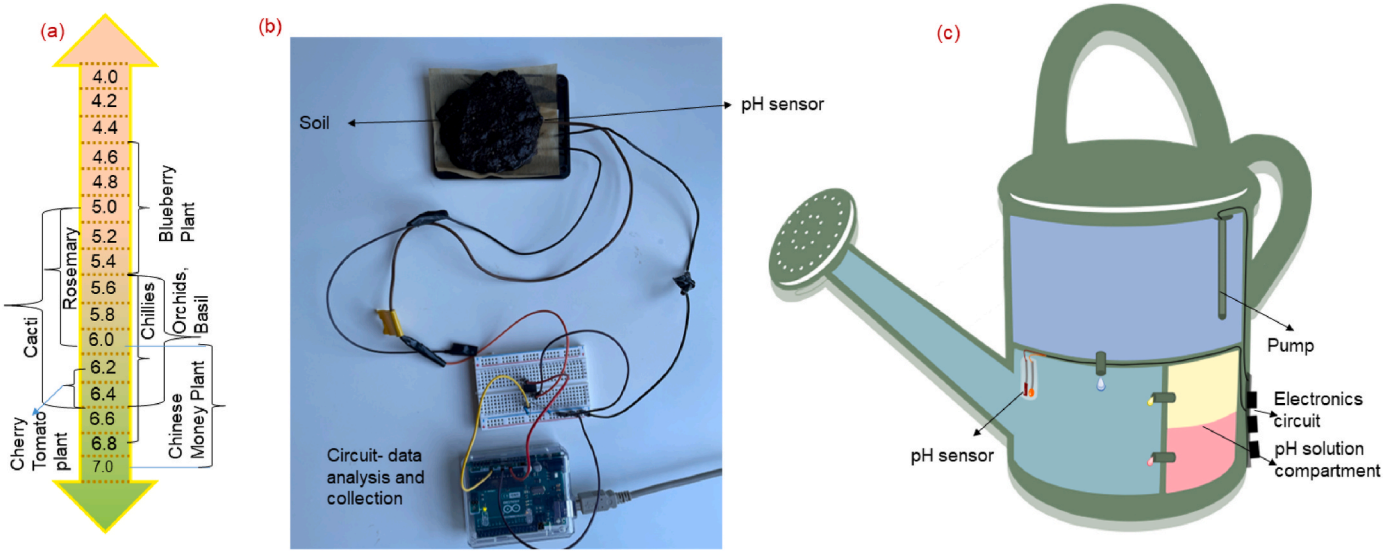

Fig. 1. (a) The range of pH values for different plants (b) soil monitoring system (c) schematic representation of the watering can with sensors and circuits for controlling the pH value of water.

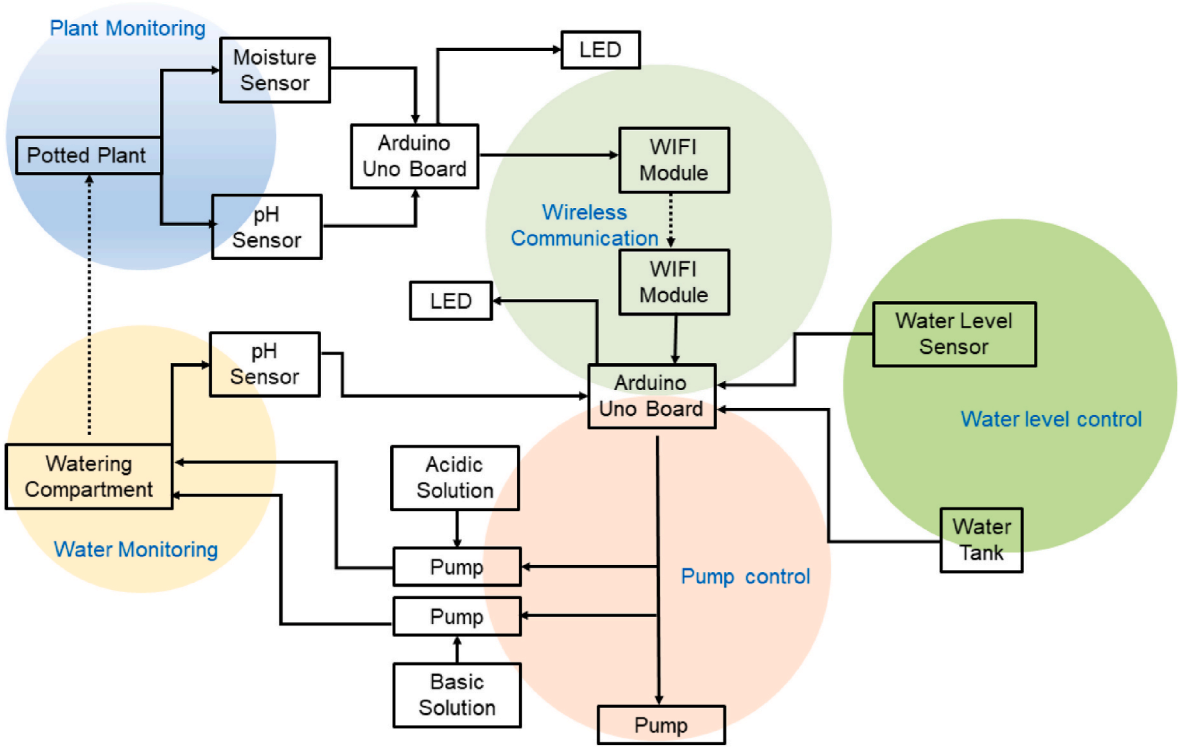

Fig. 2. Schematic diagram of system architecture for smart watering can with the sensor in potted plant.

These acid and base solutions were chosen as they are suitable for hydroponic systems, and, thus, will cause no harm to the plant. The interference of sensitive electrodes to other ions including $Ca_3(NO_3)_2$, KCl, $MgCl_2$, NaCl, and NH_4NO_3 at 0.01 M concentration in temperature 21.7 °C were carried out using RuO_2 SE with glass-based Ag/AgCl RE. Furthermore, we also carried out a detailed electrochemical property of the SE with various REs using EIS and CV by 3 electrode system with Gamry potentiostat (Interface 1010E). The EIS analysis was obtained from 1 MHz to 0.1 Hz and CV in the potential range −0.8 V to 0.8V in the scan rate 100 mV/s in pH 7 solution.

2.2. Data analysis and prediction

The calibration of the electrodes required a simple amplifying circuit to increase the range of the potential difference values read by the Arduino Uno microcontroller. The amplifying circuit makes use of a rail-to-rail operational amplifier in a non-inverting configuration. From previous data, the potential difference between the SE and RE is expected to fall in a range of 0–600 mV for solutions with pH 4–8 on the pH scale. The analog input/output pins of the Arduino board can tolerate a negative voltage of no more than 0.5 V. Because of this, a non-inverting configuration was the most straightforward choice for the amplifying circuit. On the other hand, the microprocessor can safely read positive voltages up to 5 V. To allow room for error, and additional measurements, the gain of the amplifier was limited. To avoid supplying voltages close to 5 V for extended periods of time, the maximum input voltage to the circuit was considered to be 500 mV, which allows for measuring the performance of electrodes in solutions with a lower pH value than 4. Furthermore, it was decided that this maximum voltage should correspond to an amplified signal of 4 V, again, for safety reasons as the system required continuous readings at the analog pins. Thus, the gain of the amplifier should be equal to 8. The gain of a non-inverting amplifier depends on the resistor values (Gain = 1+ (R_2/R_1) in the feedback circuit. This means that the expected ratio between the two resistors is 7. Due to the range of resistors available as well as the requirement that such resistors be in the kΩ range - so as to not overload the operational amplifier with a high current - R_2 was chosen as 6.8 kΩ and R_1 was chosen as 1 kΩ, resulting in an overall gain of 7.8. Once the signal was amplified, it could be read by the analog input pins of the Arduino Uno board. As this particular microprocessor has a 10 bit analog-to-digital converter, this means that it can read 2^{10} values in its range of tolerance, which is 0–5 V. Therefore, the input voltage is read as an integer value between 0 and 1023, where 0 equals 0 V, while 1023 equals 5 V. In order to display the read value in volts, the following formula is used.

$$V = V_{IN} * \frac{5}{1024} \quad (1)$$

This formula is then used in the Arduino program, which acts as a digital voltmeter, by reading the output value from the amplifier circuit, and then printing it as a voltage to the monitor. The output of the amplifier is connected to the analog pin A0 on the board, which is set as an input. In the code, the integer variable, input, is the incremental value between 0 and 1023 read at the pin, while the float variable, V, is the equivalent voltage printed to screen. As the emf between the electrodes is ultimately intended to be measured with an Arduino, the tests were adjusted and repeated. The analog inputs of the Arduino Uno have an analog-to-digital resolution of 10 bits, which means that they return values between 0 and 1023, which correspond to a potential difference between 0 V and 5 V, respectively. Consequently, the resolution of the analog inputs is 4.9 mV. Therefore, to increase the reliability of the measurements taken, the signal from the electrodes was connected to an amplifier with a gain of 7.8 as a means to expand the range of input values. The experiment was repeated, resulting in new linear equations for the electrode pairs.

2.3. Soil monitoring

The aim of the soil tests was to determine whether the electrodes would perform well in conditions where they were not fully submerged in a liquid solution. The electrodes were attached to alumina substrate, placed in a plastic container, and covered with semi-permeable filter paper. The reason for this was to provide the electrodes with a firm base,

such they could not be bent or damaged by the weight of the soil, and to provide a barrier between the solid particles of the soil and the electrodes. By using filter paper, only the liquid solution from the soil would come into contact with the electrodes. It was found that for both types of REs, Ag/AgCl and carbon based, there is no electrical connection between the sensitive and reference electrodes unless they are connected by a continuous layer of water. The experiments were carried out in a single soil. Initially, dry soil was placed on top of the electrodes and the voltage was measured. Due to the lack of water, there was no path for current to flow between the electrodes, resulting in open circuit conditions. The water content of the soil gradually increased, and the voltage measured, which lead to the conclusion that stable and reliable measures can only be taken when the soil is saturated with water. Once it was determined that saturation was essential for an accurate measurement, the electrodes were tested under soil conditions. These experiments required that the electrodes be placed under saturated soil, after which the potential difference was measured for 30 min, at an interval of 4 s. First, the electrodes were tested by saturating the soil with clean tap water. The same sample of soil was then saturated with an acidic and basic solution. The pH was adjusted using commercial phosphoric acid and potassium hydroxide as in the previous experiments. In this experiment, the potential difference was measured at the analog input pins of the Arduino Uno. Because of this, the electrodes were connected to the aforementioned amplifier circuit with a gain of 7.8.

2.4. Real-time test and automated system in watering can

The performance of the electrodes in real-time conditions was tested by carefully placing them in the soil of the potted plant in a vertical position. The plant was then watered to saturation, and the measurements were taken with the help of the Arduino and the amplifier circuit. The pH of the soil was then measured again, after the plant was watered with an acidic solution containing phosphoric acid. The proposed automated watering can system consists of two parts – a sensor circuit attached to the plant to be monitored, and the automated water can, as shown in Fig. 1c and the schematic of system architecture given Fig. 2. The electrodes measure the pH of the soil using the method described in the real time experiment. The moisture of the soil is also measured. This information is then sent to the automated watering can, where a solution is prepared. Depending on the size of the pot, and the moisture level of the soil in it, the program calculates the appropriate amount of water the plant needs, and then, using a submerged water pump, transports it to a separate container with an opening to the outside environment. The pH of this solution is also regulated to an appropriate level depending on the plant type. The pH of the watering solution is adjusted using two peristaltic, or dripping, pumps. The system works such that once the water is transported into the separate container, its pH is measured using an electrode pair. Then, if the pH of the water is not in an optimal range, its pH is adjusted by transferring a small amount of acidic or basic solution into a separate container. The pH is then measured again, and the process is repeated until the solution is in an appropriate range. To protect the submerged water pump, a moisture sensor is used as a water level sensor in the water tank. The program can, thus, ensure that the water pump will not be turned on unless there is enough water in the reserves.

3. Results and discussion

3.1. Sensor calibration and mechanism

Fig. 3a shows the schematic of the potentiometric pH sensor used in this work, which was fabricated using screen-printing method [23,24]. The sensor was tested initially in water to achieve the calibration and then tested in soil as shown in Fig. 3b and c. Electrode sensitivity was determined by sweeping the electrode through different pH values and measuring the resulting emf. Prior to measuring in soil, the potentiometric performances of the pH sensors based on both Ag/AgCl and carbon REs with RuO_2 SE were tested in distilled water. In this case, tap water was used as it is assumed that tap water is commonly used for watering plants, and therefore, determining the electrode's performance in these conditions is of great importance. Initially, the emf between the SEs and the REs was measured using a multimeter and then with a designed circuit using Arduino Uno board. The potential difference was measured for pH values 3–8, as this is the pH range suitable for most plants (as shown in Fig. 1a). The performance of the electrodes in real-time conditions was tested by carefully placing them in the soil of the potted plant in a vertical position, image given in Fig. 3c. In addition to the pH sensor, to measure the moisture content of the soil, a capacitive probe-based humidity sensor was used. The moisture sensor was directly connected to the Arduino Uno board and calibrated. The measured moisture variations are given in Fig. 4 and is represented in integer (manufacturer instructions to determine the sets of the value range in which the soil was deemed dry (570, 380), wet (380, 190), and very wet (190, 0)).

The difference in emf for various pH values for the RuO_2 SE and the

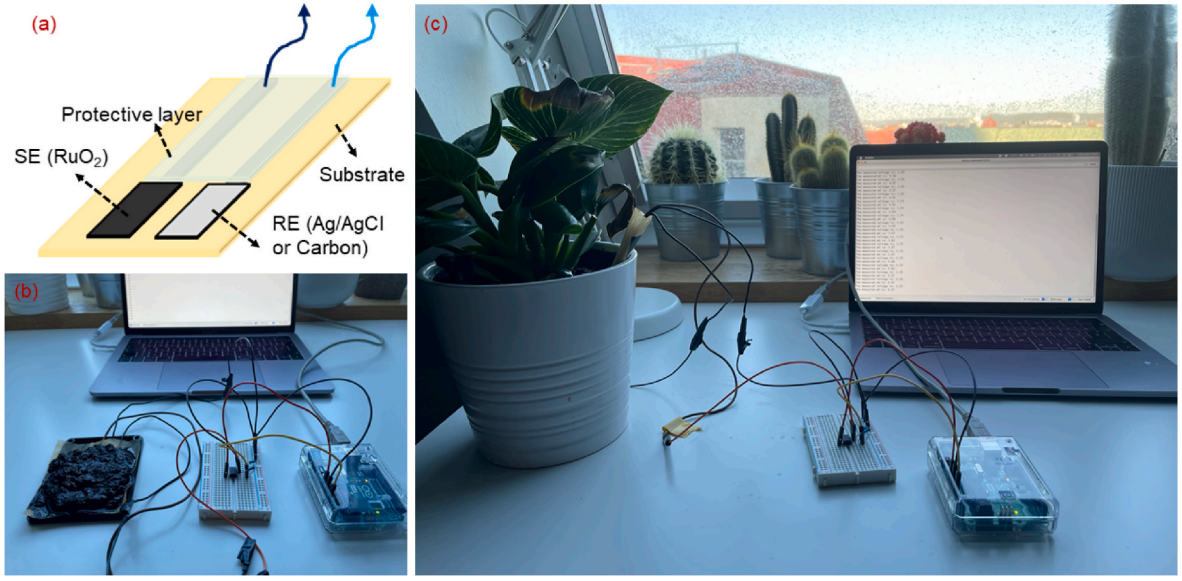

Fig. 3. (a) Schematic of potentiometric pH sensor (b) image of pH sensor measured in soil and (c) image of the sensor with circuit in potted plant for data analysis.

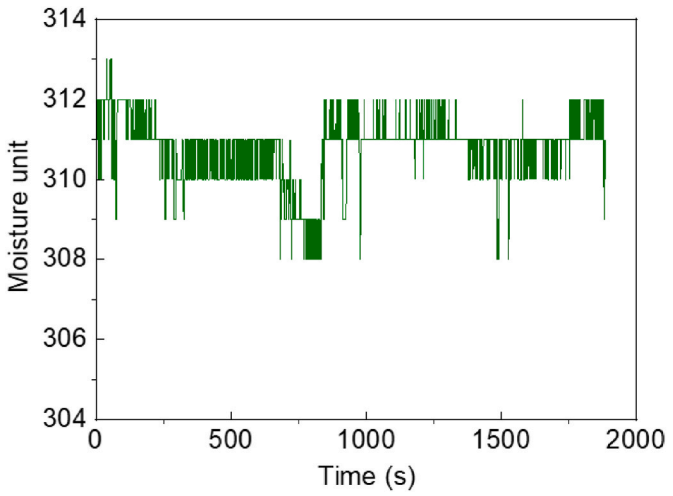

Fig. 4. Long-term moisture monitoring of potted plant.

Ag/AgCl RE, measured using a multimeter, are given in Fig. 5a. In the range of pH 3–8, the sensor shows near Nernstian response with a sensitivity or slope factor of 52.68 ± 2.16 mV/pH and standard potential (E_0) of 477.76 ± 12.53 mV. On the other hand, the sensitivity of the sensors in the pH range 5–8 is 59.16 ± 1.65 mV/pH ($R^2 = 0.9969$) with the E_0 value equal to 522.50 ± 10.89 mV/pH. These sensitivity factors were very close to the theoretical Nernst equation (59.14 mV/pH) between pH and cell potential. We noted that by changing the pH range of the solution the sensitivity of the electrode varies due to different hydration responses of the sensor in acidic and alkaline regions, as confirmed in previous works [25]. Even though we used a quasi RE (without KCl layer) the observed sensitivity 52.68 ± 2.16 mV/pH of the screen-printed sensor is similar to the reported screen printed based pH sensors with screen printed Ag/AgCl reference electrode with KCl layer [25] as well as commercial glass Ag/AgCl/KCl reference electrode [24]. This similarity may be because the role of KCl in a standard reference electrode is the provision of a small liquid junction potential which is probably provided by the Cl^- ions dissociating slowly and stably from hand-printed AgCl layer. This may eliminate the requirement of a KCl layer under the circumstances described in this study. Low volume of testing sample, simplicity of fabrication, disposability and stability are the common reasons for using quasi-RE. However, if required, there are many recommended methods to effectively introduce KCl into the fabrication procedure of planar electrochemical sensors [26]. The experiment was then repeated using an amplifier circuit with a gain of 7.8 and measured using an Arduino Uno board. The sensitivity of the sensor after adding a gain circuit was observed to be 0.4179 V/pH or 417.9 mV/pH. This is comparable to the previously obtained sensitivity when dividing by 7.8, being 53.577 mV/pH. The newly obtained result shows a 1.7% increase compared the value obtained from the measurement with a multimeter.

A similar potentiometric experiment was carried out using a carbon based RE. The sensor shows a sensitivity of 42.33 ± 1.26 mV/pH and a standard potential (E_0) of 547.44 ± 7.62 mV. A similar characterization was also carried out by using the Arduino Uno board and the sensitivity was 328.4 mV/pH. This is equal to 42.103 mV/pH after considering the gain value. Hence, we noticed that when compared to the Ag/AgCl based RE, the SE electrode with carbon printed RE shows a lower sensitivity. This could be due to surface reactions of the conductive RE compared to the Ag/AgCl RE. It was observed that due to its high electrical double layer capacitance and inertness in different solutions, carbon materials have been successfully employed as quasi-REs in applications such as concrete, electrochemical scanning tunnelling microscopy and supercapacitors [27–29]. However, at pH lower than 5 or 6 the measured emf decreases, indicating that surface reactions might

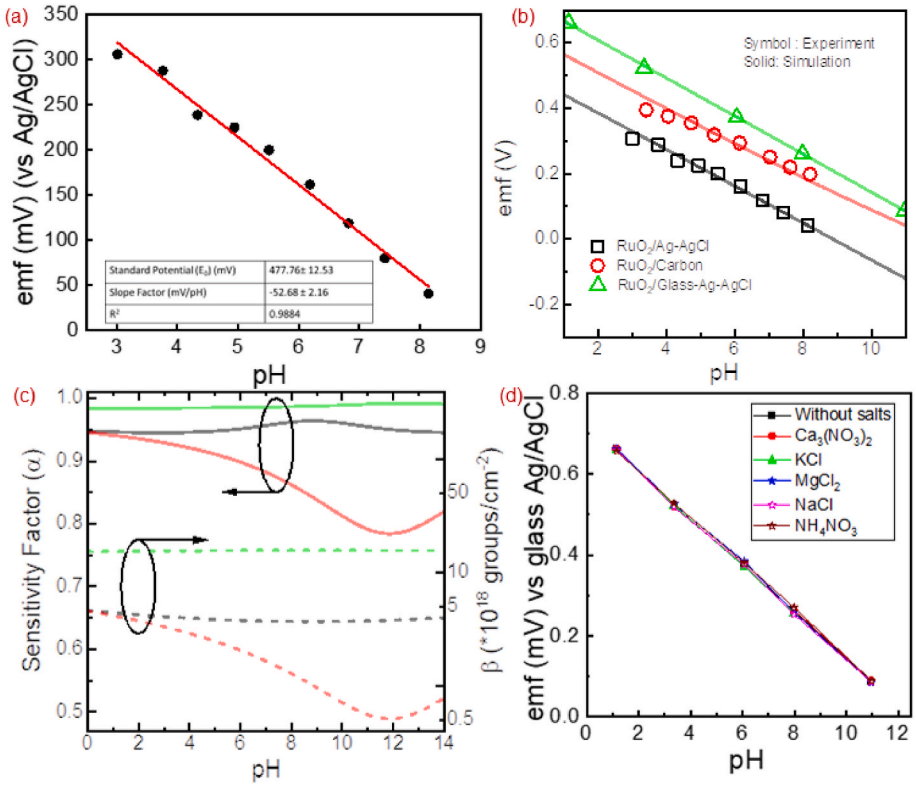

Fig. 5. Potentiometric sensing performances of the thick film pH sensor in the range of pH 3 to 8 (a) emf value of the sensor measured using a multimeter (inset pH sensing performances in pH 5 to 8) for RuO_2 with printed Ag/AgCl RE (b) experimentally measured and simulated surface potential (c) sensitivity parameter and intrinsic buffer capacity [same color notations] for oxide and different reference electrodes (d) Interference of SE in different salt solutions.

disturb the carbon ability to produce stable results in highly acidic conditions, decreasing the pH sensor sensitivity in the pH range 3–9.

Further studies on modelling and simulations based on obtained above results were carried out to understand the difference in sensing mechanism. Fig. 5b presents the comparison of potentiometric performances of RuO_2 vs glass based commercial Ag/AgCl RE, RuO_2 vs printed Ag/AgCl RE and RuO_2 vs printed carbon RE. For proper simulation and proof-of-concept, it is necessary to work with the dissociation constants and surface states for the oxide-electrolyte interactions. The experimental data is used to extract the RuO_2 affinities (pK1 and pK2) for protonation and deprotonation for a specific value of surface states (N_S) [30,31]. The obtained surface potential is used to calculate the zeta potential with a stern capacitance of $0.8.m^{-2}$ [32] which is then converted to the charge density from the Gouy-Chapman-Stern equation. The charge affinities and surface states are calculated from the surface charge density using the Site-Binding method [33]. The extracted material properties are utilized to calculate the surface potential with self-consistency for minimal error. The extracted values of pK1, pK2 and N_S are 7.8241, 9.87 and 10^{19} cm^{-2} for RuO_2 Vs Ag–AgCl as RE. The isoelectric point for RuO_2/Ag–AgCl system is found to be a little bit higher than the bare RuO_2 due to the higher protonation of screen-printed electrode. With the consideration of carbon and glass/-Ag–AgCl as a RE, the measured surface potential is higher than the Ag–AgCl electrode due to the extra surface states from the electrode with a higher affinity of deprotonation leading to a negative bias at the RE [34]. The calculated values of pK1, pK2, N_S are 9.7445, 14, 1.5×10^{19} cm^{-2} and 12.0494, 12.81, 1.5×10^{19} cm^{-2} for RuO_2/Carbon and RuO_2/Glass-Ag-AgCl as a system respectively. Other than surface potential, sensitivity factor (α) and intrinsic buffer capacity (β) are the two parameters that define the effectiveness of the oxide-electrolyte interactions. α and β can be calculated as [35];

$$\alpha = \frac{1}{\frac{2.303 k_B T C_{diff}}{q^2 \beta} + 1} \tag{2}$$

$$\beta = \frac{d\sigma_o}{d\mathrm{pH}_s} \tag{3}$$

$$\text{where, } \sigma_o = -Q_0 \, sinh\left(\frac{q\Psi_o}{2k_B T}\right) \tag{4}$$

$$Q_0 = \sqrt{8 k_B T \varepsilon_w I_0 N_{avo}} \tag{5}$$

$$\sigma_o = qNs\left(\frac{H_S^2 - K_1 * K_2}{H_S^2 + H_S * K_1 + K_1 * K_2}\right) \text{ [from Site} - \text{Binding Method]} \tag{6}$$

where, k_B, T, C_{diff}, q, σ_o, Ψ_o, I_o, N_{avo}, ε_w, H_s and pH_S are Boltzmann constant, temperature, differential capacitance, electronic charge, surface potential, electrolyte concentration, Avogadro number, electrolyte permittivity, surface hydrogen ion concentration and surface pH. The sensitivity factor (α) and intrinsic buffer capacity (β) are highest for the RuO_2/Glass-Ag-AgCl (as shown in Fig. 5c) due to the increased slope and reactivity of silanol sites with the change in bulk pH. The decrement of the surface charge density with the surface pH is the reason behind the lowest value of α and β for RuO_2/Carbon. Thus, the calculated material properties of the system pave the way for designing new architectures for ISFETs using RuO_2 as the molecule interacting site.

Further, the influence of SE interferences to other ions was also tested by using pH RuO_2 SE with standard glass-based Ag/AgCl RE in a solution of $Ca_3(NO_3)_2$, KCl, $MgCl_2$, NaCl, and NH_4NO_3. These salts were particularly chosen for this study because sodium (Na^+), potassium (K^+), magnesium (Mg^+), ammonium (NH_4^+) and calcium (Ca^+) are macronutrients and essential soil base cations which play a critical role in the soil-nutrient relationship [36]. Sodium (Na^+) is a non-essential base cation which participates in exchange reactions along with the other base cations and acts as a buffer against acidity fluctuations in the soil [36]. It is therefore vital that a sensor that was fabricated for application in soil pH monitoring is not significantly affected by the interference effect produced by any of these ions. The potentiometric performances of the sensor in various salt solutions are given in Fig. 5d and performances deviation in slope factor is given in Table 1. It was noted that the sensor shows ±1 mV/pH sensitivity variations which is comparatively negligible. RuO_2 shows an almost instantaneous response time within the pH range applied in this study (pH 3–8, Fig. 1a) with a little higher response time expected at pH 8 because of the slightly higher concentration of OH^- ions that are bigger in size than H^+ ions and therefore diffuse more slowly into the sensing layer [37]. Additionally, RuO_2 electrodes are stable over a long period of time without any significant change in sensitivity and exhibit excellent adhesion of the glass containing RuO_2 layer to the substrate [24]. This implies that when applied in soil for pH monitoring, fabricated sensors can last up to weeks without replacement and do not risk leaching of the sensing layer into the soil if it were to come in direct contact with it.

The EIS analysis of the RuO_2 electrode with glass and printed Ag/AgCl and carbon-based REs were carried out in pH 7 solution. The Nyquist and Bode phase angle plots are shown in Fig. 6a and b respectively. It can be observed that even though the REs showed different sensitivities and emf results against the RuO_2 SE, the electrochemical reaction taking place on the electrodes is very similar behaviour. The Nyquist plot presents a slightly curved line in the low-frequency range suggesting an ionic adsorption/desorption at the metal oxide/solution interface and an incomplete semi-circle in the high-frequency range due to the charge transfer process. The bulk resistance of the material causes the charge transfer resistance in high frequency range while the ionic diffusion causes the straight line in the low frequency range. However, when comparing the measurement with previous studies on 2 electrodes system using the interdigitated electrode, it was noticed a large semi-circle arc in the low frequency range [38]. This reveals that the measurement system and the electrode configuration influence the measured impedance. The EIS confirms that both ionic exchange and charge transfer processes are involved in the sensing mechanism [38]. However, it was observed that by changing the REs the impedance value of the sensor varied. The Bode phase angle and impedance plot confirmed the capacitive nature of the electrode due to ionic diffusion. The mixed ionic and electronic conductivity of the RuO_2 electrode is responsible for its pH sensing performances [38].

This behaviour is confirmed in the CV at pH 7 (Fig. 6c). RuO_2 is a reactive material both in its amorphous and crystalline phases. The several faradaic peaks observed in the CV are due to the electron transfers processes from proton (H^+) coupling [39]. These peaks also demonstrate some of the different oxidation states of Ru, which can range from Ru(II) to Ru(VI) [40]. RuO_2 also presents pseudo-capacitive properties, and even in the presence of a counter electrode a large non-faradaic current is observed. Interestingly, all REs showed a similar performance, with the carbon based RE being more similar to the commercial glass Ag/AgCl electrode than the printed Ag/AgCl, which had the peaks shifted to the left. This could indicate that the carbon RE is potentially more stable for certain electrochemical techniques than for others. The large double-layer capacitance and low reactivity carbon materials (as shown in Fig. 5c) could be positive parameters to consider in certain situations against printed Ag/AgCl REs. However, it presented

Table 1
Comparison of performances of SE with interference to different salts.

Salts	Sensitivity (mV/pH)	R^2 value	Deviation (%)
Without	58.29	0.9997	0
$Ca_3(NO_3)_2$	57.92	0.0992	−0.63
KCl	58.61	0.9995	0.55
$MgCl_2$	58.72	0.992	0.74
NaCl	58.22	0.993	−0.12
NH_4NO_3	57.54	0.995	−1.29

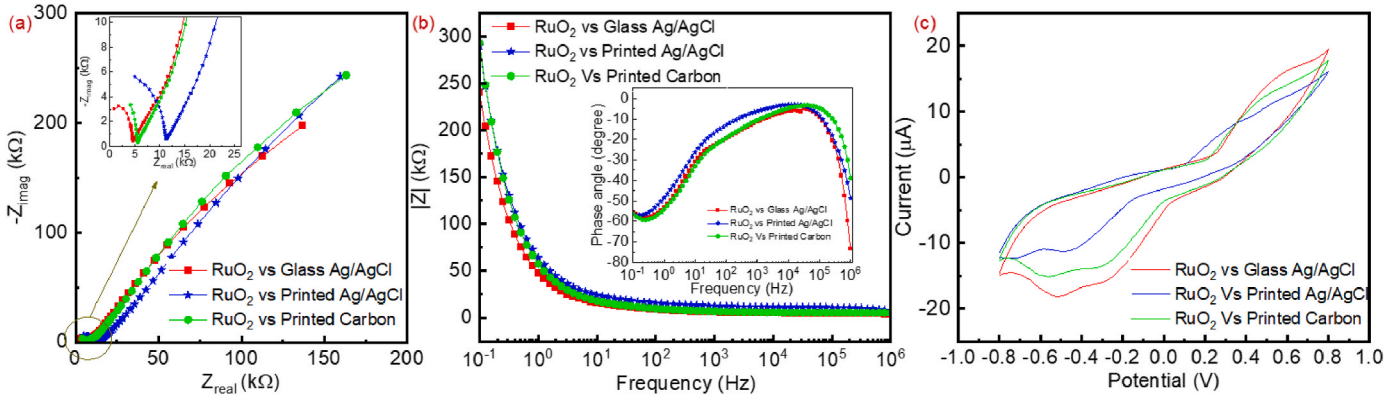

Fig. 6. Comparison of RuO_2 SE with different RE in pH 7 solution (a) Nyquist Plot (b) Bode phase angle plot and (c) CV curve.

a lower sensitivity when it came to the potentiometric sensor, indicating that the large double-layer formation might hinder the potential difference between the SE and the carbon-based RE.

3.2. Soil testing

The performance of the electrodes was measured at three pH levels, by saturating the water with three different solutions. Initially, the soil was saturated with a solution with a pH value of 8.5. In this case, this was clean tap water. Then, the solution was adjusted to measure 6.5 on the pH scale, and the soil was saturated again. Finally, the same procedure was repeated for a solution of 4.0 on the pH scale. These three values were specifically chosen as, commonly, plants cannot thrive in soils of pH lower than 4.0 or higher than 8.5. It must be noted that different plant species thrive in different pH levels as given in Fig. 1a. Therefore, it was deemed important to determine the electrodes' performance in both acidic and basic pH range. The potentiometric performances of RuO_2 with Ag/AgCl were shown in Fig. 7a. For water with a pH value of 8.5 the sensor showed emf of 389.5 mV and when we consider this value, the saturated pH value of soil is 7.64. Similarly for pH 6.5 and pH 4 of watering solution after considering the measured voltage from Fig. 7a, the saturated pH value of soil is 7.17 and 7.01. It is important to note, however, that when saturated with a constant pH solution, the pH of the soil is not expected to change to the same pH of the solution as there are many factors and chemical reactions within the soil that affect its pH. In our measurement we started with basic solution saturation and gradually added the acidic solution. So already existing basic solutions dilute the acidity of solution and finally affect the pH value of soil. In addition to this, another one of the factors is the buffering capacity of soil which explains soil's ability to resist changes in pH. Different types of soils have different buffering capacities. Clay soil is the most resistant to changes in pH, loam soil less so, while sandy soils are least resistant. In turn, the buffering capacity of a soil depends on several factors. A soil's buffering capacity is affected by the carbonate content in the soil. For non-carbonate containing soils, the buffering capacity is directly proportional to initial pH, clay content, cation exchange capacity, and exchangeable sodium concentration. Whereas, in carbonate containing soils, the buffering capacity is directly proportional to the cation exchange capacity, carbonate content and exchangeable sodium concentration; and inversely proportional to initial pH and clay content [41]. Therefore, it is important to know, that these experiments do not take into account the chemical contents of the soil, and thus do not seek to determine how much acidic or basic solution is required to achieve a predetermined pH value for the soil of the plant.

The results of the real-time tests can be seen in the videos provided (SV1 and SV2). When watered with tap water, the pair of the sensitive electrode and the first silver chloride reference electrode returned an average value of 5.75. Similarly, the carbon-based electrode also showed an average of 5.75. The plant used in this experiment is a Philodendron Birkin, otherwise known as a Philodendron White Wave plant. Philodendrons prefer a slightly acidic, in the range of 5–6 on the pH scale, loamy soil. Because of this, it can be noted that the pH of the potted plant is well within its optimal range. In the second part of the experiment, the plant was watered with a solution at a pH level of 4.84. It can be seen in the videos, however, that this did not result in an overall change in the pH of the soil. This result is expected, as it was explained previously, that loamy soils have a moderate buffering capacity, and thus can resist smaller changes in pH. Thus, it can be concluded that the pH of potted plants cannot safely be changed instantaneously and is a long process. The difference between this experiment, and the soil tests, is that the pot soil cannot be saturated with a highly acidic solution, as was the case in the soil tests, for risk of damaging the plant. Because of this, the

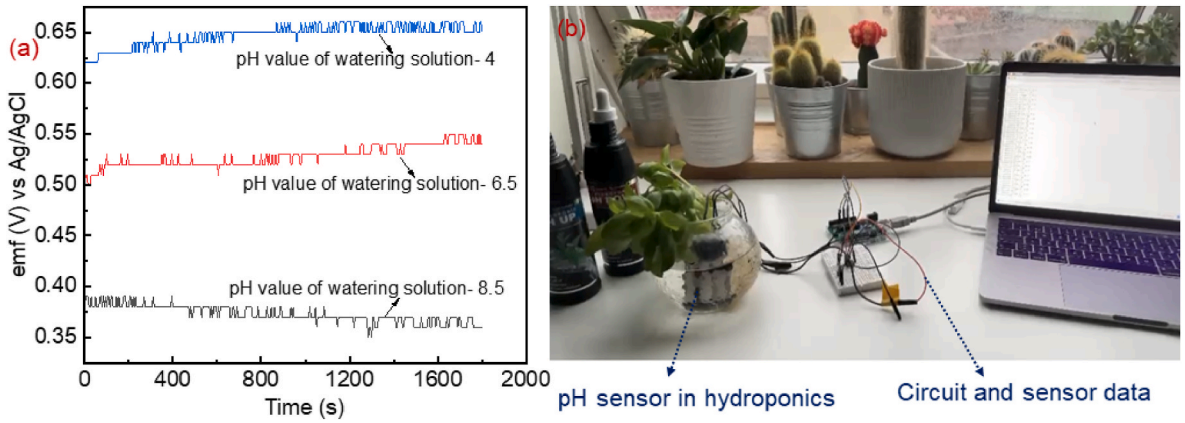

Fig. 7. (a) Performances of sensor in soil with watering solution of different pH value (b) image of pH sensor implemented for hydroponics application.

proposed system continuously monitors the soil pH of the potted plant and adjusts the solution as needed. Finally, this work carried out changing the pH value of solution of water in hydroponics, image shown in Fig. 7b and video in supporting SV3.

4. Conclusion

In summary, this work developed soil monitoring pH sensors using RuO_2 as SE and two different types of REs based on Ag/AgCl and carbon. The major advantage of carbon-based RE is less toxicity and low cost along with excellent sensing performances. When the RuO_2 is exposed to the solution, negative, neutral, or positive surface charged groups are formed on the surface of the SE depending on the pH of the solution. We carried out a detailed theoretical and experimental analysis to understand the sensing mechanism between RuO_2 vs Ag/AgCl RE and RuO_2 vs carbon RE. The experiments undertaken during this project found that when used with Ag/AgCl reference electrodes, the RuO_2 has a sensitivity of 52 mV/pH, which is an almost Nernstian response. On the other hand, when used with a carbon-based reference electrode, the sensitivity was slightly lower at 42 mV/pH. However, despite their sub-Nernstian sensitivity, carbon-based reference electrodes are important, and might be preferred due to their sustainability. By monitoring the soil moisture and pH of potted plants, it ensures that they are not under- or overwatered, and that the soil is in an optimal pH for the selected plant - and, thus, ensuring that the plant can absorb a maximum amount of necessary nutrients from the soil. The information collected from the plant soil is then used to prepare a watering solution. The amount of water the plant needs is calculated. If the plant is not in the correct pH range for its species, the pH of the water is adjusted to be within this range using phosphoric acid and potassium hydroxide solutions intended for use in hydroponic system. The result is an optimal watering solution for the plant type and soil conditions. These findings are of considerable importance as such miniature sensors could be a cost-effective, flexible and portable alternative to traditional pH measuring methods, and, as such, could be used in many applications from hydroponics to environmental monitoring. To implement this in a large area, multiple sensors are required for deployment in various locations of the soil to monitor pH values. Additionally, an online pH monitoring system is required for the water tank or reservoir. A connected sensing networking system with data gathering and analysis methods will be highly necessary and will be carried out in future work.

Credit author statement

Conceptualization: AR, RH, LM; methodology: AR, LM; software: NK, VG; evaluation; AR, KU, FF, CL, CM, LM investigation: AR, KU, FF, NK, LM; writing—original draft preparation; AR, KU, FF, NK, LM writing—review and editing, all authors; funding acquisition. FF, RH, LM; All authors have read and agreed to the published version of the manuscript.

Declaration of competing interest

The authors declare that they have no known competing financial interests or personal relationships that could have appeared to influence the work reported in this paper.

Data availability

Data will be made available on request.

Acknowledgment

This work was supported by the European Commission through the AQUASENSE (H2020-MSCA-ITN-2018-813680) project and NERC discipline hopping activities to tackle environmental challenges project (SEED-2022-317475).

Appendix A. Supplementary data

Supplementary data to this article can be found online at https://doi.org/10.1016/j.rineng.2023.101297.

References

[1] S. Hussain, A. Amin, M. Mubeen, T. Khaliq, M. Shahid, H.M. Hammad, S. R. Sultana, M. Awais, B. Murtaza, M. Amjad, S. Fahad, K. Amanet, A. Ali, M. Ali, N. Ahmad, W. Nasim, Climate smart agriculture (CSA) technologies, in: W.N. Jatoi, M. Mubeen, A. Ahmad, M.A. Cheema, Z. Lin, M.Z. Hashmi (Eds.), Building Climate Resilience in Agriculture: Theory, Practice and Future Perspective, Springer Inter. Publishing, Cham, 2022, pp. 319–338.

[2] Y. Liu, C. Bachofen, R. Wittwer, G. Silva Duarte, Q. Sun, V.H. Klaus, N. Buchmann, Using PhenoCams to track crop phenology and explain the effects of different cropping systems on yield, Agric. Syst. 195 (2022), 103306.

[3] M. Raimondo, C. Nazzaro, G. Marotta, F. Caracciolo, Land degradation and climate change: global impact on wheat yields, Land Degrad. Dev. 32 (1) (2021) 387–398.

[4] K. Garrett, M. Nita, E. De Wolf, P. Esker, L. Gomez-Montano, A. Sparks, Plant pathogens as indicators of climate change, Clim. Change (2021) 499–513. Elsevier.

[5] L. Manjakkal, S. Mitra, Y. Petillo, J. Shutler, M. Scott, M. Willander, R. Dahiya, Connected sensors, innovative sensor deployment and intelligent data analysis for online water quality monitoring, IEEE Internet Things J. 8 (2021) 13805–13824.

[6] B. Chugh, S. Thakur, A.K. Singh, R. Joany, S. Rajendran, T.A. Nguyen, Electrochemical Sensors for Agricultural Application, Nanosensors for Smart Agriculture, Elsevier, 2022, pp. 147–164.

[7] A.J. Bandodkar, W.J. Jeang, R. Ghaffari, J.A. Rogers, Wearable sensors for biochemical sweat analysis, Annu. Rev. Anal. Chem. 12 (2019) 1–22.

[8] M. Bariya, H.Y.Y. Nyein, A. Javey, Wearable sweat sensors, Nature Electronics 1 (3) (2018) 160–171.

[9] A. Subeesh, C.R. Mehta, Automation and digitization of agriculture using artificial intelligence and internet of things, Artif. Intel. Agr. 5 (2021) 278–291.

[10] M.T. Linaza, J. Posada, J. Bund, P. Eisert, M. Quartulli, J. Döllner, A. Pagani, I. G. Olaizola, A. Barriguinha, T. Moysiadis, Data-driven artificial intelligence applications for sustainable precision agriculture, Agronomy 11 (6) (2021) 1227.

[11] C. Pylianidis, S. Osinga, I.N. Athanasiadis, Introducing digital twins to agriculture, Comput. Electron.in Agr. 184 (2021), 105942.

[12] M.Z. Mehmood, M. Ahmed, O. Afzal, M.A. Aslam, R. Zoq-ul-Arfeen, G. Qadir, S. Komal, M.A. Shahid, A.A. Awan, M.A. Awale, A. Sameen, T. Kalsoom, W. Nasim, Fayyaz-ul-Hassan, S. Ahmad, Internet of things (IoT) and sensors technologies in smart agriculture: applications, opportunities, and current trends, in: W.N. Jatoi, M. Mubeen, A. Ahmad, M.A. Cheema, Z. Lin, M.Z. Hashmi (Eds.), Building Climate Resilience in Agriculture: Theory, Practice and Future Perspective, Springer International Publishing, Cham, 2022, pp. 339–364.

[13] A.K. Pandey, A. Mukherjee, A review on advances in IoT-based technologies for smart agricultural system, in: P.K. Pattnaik, R. Kumar, S. Pal (Eds.), Internet of Things and Analytics for Agriculture, Springer Singapore, Singapore, 2022, pp. 29–44, lume 3.

[14] S.G. Lemos, A.R.A. Nogueira, A. Torre-Neto, A. Parra, J. Alonso, Soil calcium and pH monitoring sensor system, J. Agr. food chem. 55 (12) (2007) 4658–4663.

[15] J. Artigas, A. Beltran, C. Jiménez, A. Baldi, R. Mas, C. Domınguez, J. Alonso, Application of ion sensitive field effect transistor based sensors to soil analysis, Comput. Electron. Agric. 31 (3) (2001) 281–293.

[16] J.M. Margarit-Taulé, M. Martín-Ezquerra, R. Escudé-Pujol, C. Jiménez-Jorquera, S.-C. Liu, Cross-compensation of FET sensor drift and matrix effects in the industrial continuous monitoring of ion concentrations, Sensor. Actuator. B Chem. 353 (2022), 131123.

[17] F.M. Seaton, G. Barrett, A. Burden, S. Creer, E. Fitos, A. Garbutt, R.I. Griffiths, P. Henrys, D.L. Jones, P. Keenan, Soil health cluster analysis based on national monitoring of soil indicators, Eur. J. Soil Sci. 72 (6) (2021) 2414–2429.

[18] E. Saljnikov, A. Lavrishchev, J. Römbke, J. Rinklebe, C. Scherber, B.-M. Wilke, T. Tóth, W.E.H. Blum, U. Behrendt, F. Eulenstein, W. Mirschel, B.C. Meyer, U. Schindler, K. Urazaliev, L. Mueller, Understanding and monitoring chemical and biological soil degradation, in: E. Saljnikov, L. Mueller, A. Lavrishchev, F. Eulenstein (Eds.), Advances in Understanding Soil Degradation, Springer Int. Publishing, Cham, 2022, pp. 75–124.

[19] S.O. Oshunsanya, Introductory Chapter: Relevance of Soil pH to Agriculture, Soil pH for Nutrient Availability and Crop Performance, 2018. IntechOpen.

[20] S. Kumar, R.T. Babankumar, M. Kumar, Soil pH sensing techniques and technologies, International J. Adv. Res. Elect. Electron. Inst. Eng. 4 (5) (2015).

[21] F.G. Fernández, R.G. Hoeft, Managing soil pH and crop nutrients, Illinois agronomy handbook 24 (2009) 91–112.

[22] K. Zhalnina, R. Dias, P.D. de Quadros, A. Davis-Richardson, F.A.O. Camargo, I. M. Clark, S.P. McGrath, P.R. Hirsch, E.W. Triplett, Soil pH determines microbial diversity and composition in the park grass experiment, Microb. Ecol. 69 (2) (2015) 395–406.

[23] L. Manjakkal, K. Cvejin, J. Kulawik, K. Zaraska, D. Szwagierczak, A low-cost pH sensor based on RuO2 resistor material, Nano Hybrids 5 (2013) 1–15.

[24] K. Uppuluri, M. Lazouskaya, D. Szwagierczak, K. Zaraska, M. Tamm, Fabrication, potentiometric characterization, and application of screen-printed RuO2 pH electrodes for water quality testing, Sensors 21 (16) (2021) 5399.

[25] L. Manjakkal, B. Synkiewicz, K. Zaraska, K. Cvejin, J. Kulawik, D. Szwagierczak, Development and characterization of miniaturized LTCC pH sensors with RuO2 based sensing electrodes, Sensor. Actuator. B Chem. 223 (2016) 641–649.
[26] U. Guth, F. Gerlach, M. Decker, W. Oelßner, W. Vonau, Solid-state reference electrodes for potentiometric sensors, J. Solid State Electrochem. 13 (1) (2009) 27–39.
[27] Y. Abbas, W. Olthuis, A. van den Berg, Activated carbon as a pseudo-reference electrode for electrochemical measurement inside concrete, Construct. Build. Mater. 100 (2015) 194–200.
[28] A. Auer, J. Kunze-Liebhäuser, A universal quasi-reference electrode for in situ EC-STM, Electr. Commun. 98 (2019) 15–18.
[29] M. Widmaier, B. Krüner, N. Jäckel, M. Aslan, S. Fleischmann, C. Engel, V. Presser, Carbon as quasi-reference electrode in unconventional lithium-salt containing electrolytes for hybrid battery/supercapacitor devices, J. Electrochem. Soc. 163 (14) (2016) A2956–A2964.
[30] M. Kosmulski, Isoelectric points and points of zero charge of metal (hydr) oxides: 50 years after Parks' review, Adv. coll. interf. sci. 238 (2016) 1–61.
[31] Y. Lee, J. Suntivich, K.J. May, E.E. Perry, Y. Shao-Horn, Synthesis and activities of rutile IrO2 and RuO2 nanoparticles for oxygen evolution in acid and alkaline solutions, J. Phys. Chem. Lett. 3 (3) (2012) 399–404.
[32] R. Van Hal, J. Eijkel, P. Bergveld, A general model to describe the electrostatic potential at electrolyte oxide interfaces, Adv. coll. interf. sci. 69 (1–3) (1996) 31–62.
[33] A. Bandiziol, P. Palestri, F. Pittino, D. Esseni, L. Selmi, A TCAD-based methodology to model the site-binding charge at ISFET/electrolyte interfaces, IEEE Trans. Electron. Dev. 62 (10) (2015) 3379–3386.
[34] Y. Gu, D. Li, The ζ-potential of glass surface in contact with aqueous solutions, J. coll. interf. sci. 226 (2) (2000) 328–339.
[35] C. Medina-Bailon, N. Kumar, R.P.S. Dhar, I. Todorova, D. Lenoble, V.P. Georgiev, C. Pascual García, Comprehensive analytical modelling of an absolute pH sensor, Sensors 21 (15) (2021) 5190.
[36] R.W. Lucas, J. Klaminder, M.N. Futter, K.H. Bishop, G. Egnell, H. Laudon, P. Högberg, A meta-analysis of the effects of nitrogen additions on base cations: implications for plants, soils, and streams, For. Ecol. Manag. 262 (2) (2011) 95–104.
[37] G.E. Likens, C.T. Driscoll, D.C. Buso, T.G. Siccama, C.E. Johnson, G.M. Lovett, T. J. Fahey, W.A. Reiners, D.F. Ryan, C.W. Martin, S.W. Bailey, The biogeochemistry of calcium at hubbard brook, Biogeochemistry 41 (2) (1998) 89–173.
[38] L. Manjakkal, E. Djurdjic, K. Cvejin, J. Kulawik, K. Zaraska, D. Szwagierczak, Electrochemical impedance spectroscopic analysis of RuO2 based thick film pH sensors, Electrochim. Acta 168 (2015) 246–255.
[39] S. Chalupczok, P. Kurzweil, H. Hartmann, C. Schell, The redox chemistry of ruthenium dioxide: a cyclic voltammetry study—review and revision, Int. J. Electrochem. 2018 (2018), 1273768.
[40] D. Majumdar, T. Maiyalagan, Z. Jiang, Recent progress in ruthenium oxide-based composites for supercapacitor applications, Chemelectrochem 6 (17) (2019) 4343–4372.
[41] W. Luo, P.N. Nelson, M.-H. Li, J. Cai, Y. Zhang, Y. Zhang, S. Yang, R. Wang, Z. Wang, Y. Wu, Contrasting pH buffering patterns in neutral-alkaline soils along a 3600 km transect in northern China, Biogeosciences 12 (23) (2015) 7047–7056.